Biomass and Bioenergy 183 (2024) 107166

Contents lists available at ScienceDirect

Biomass and Bioenergy

journal homepage: www.elsevier.com/locate/biombioe

Hydrochar fractionation and composition in batch and continuous hydrothermal liquefaction

María J. Rivas-Arrieta [a,b], Cristian Torri [c], Alessandro Girolamo Rombolà [c], Patrick Biller [a,b,*]

[a] Aarhus University Centre for Circular Bioeconomy, Blichers Allé 20, 8830, Tjele, Denmark
[b] Department of Biological and Chemical Engineering, Aarhus University, Hangøvej 2, 8200, Aarhus N, Denmark
[c] Department of Chemistry "Giacomo Ciamician", University of Bologna, Via Sant'Alberto 163, 48123, Ravenna, Italy

ARTICLE INFO

Keywords:
Hydrochar
Continuous HTL
Nutrient recovery
Manure

ABSTRACT

Understanding differences in hydrochar characteristics in batch and continuous hydrothermal liquefaction (HTL) is crucial in determining suitable valorisation routes for this byproduct, given its high nutrient load and carbon sequestration potential.

This study thoroughly characterised hydrochar from batch and continuous HTL at 300, 325 and 350 °C, elucidating their main differences and shedding light on the operational parameters causing them. For this purpose, a bench-scale continuous HTL unit with in-line solids separation was commissioned. It was possible to differentiate primary and secondary char and infer their formation mechanism.

The results showed that batch hydrochar yields were higher (24–26%) than continuous (primary and secondary) char yields (15–19%). In both reactions, higher temperatures led to chars with lower carbon and nitrogen contents. The ash content of batch hydrochars was lower than that of continuous primary chars, revealing that the in-line char separator effectively removed inorganic impurities at reaction conditions and produced a cleaner biocrude. The nutrient distribution in the HTL products showed batch biocrudes were more contaminated by Na, K and Fe, while in the continuous biocrudes, only Fe was detected. Moreover, less carbon migrated to the solids from continuous HTL, indicating that removing inorganics may reduce secondary char formation.

Batch hydrochars showed a higher presence of oxygenated and nitrogenated compounds, while the continuous primary chars had a higher share of alkanes and alkenes.

These differences may imply that batch reactions may not serve as indicators, in terms of hydrochar characteristics, for HTL upscaling to industrial plants.

1. Introduction

Nutrient circularity demands their recovery from waste streams. The agricultural sector, for example, which encompasses livestock production, has the potential for nutrient reincorporation into other agricultural activities. Biological waste, such as manure, is rich in nutrients. Estimates suggest that one animal excretes 2–103 g P, 19–215 g K and 14–458 g N per day [1]. However, its composition is highly variable and may depend on the stable handling practices, animal feed, age, and environment. Currently, over 90% of the manure in the EU and UK (>1.4 billion tonnes) is directly applied to agricultural land [2]; this translates into approximately 1300 tonnes of P directly applied to land per year, contributing to nutrient losses by runoff, GHG emissions, and soil contamination by heavy metals and pathogens. Comparatively, the EU imported an average of 7 million tonnes of phosphate fertilisers between 2019 and 2021 [3]. Thus, upcycling these waste streams is crucial to tackling the demand for nutrients and sustainable practices.

Hydrothermal liquefaction (HTL) is a thermochemical conversion process that can produce sustainable biofuels from wet feedstocks; it occurs at high temperatures (280–375 °C) and pressures (10–25 MPa) in an aqueous environment. Its main product is biocrude, but it also generates aqueous, gaseous, and solid (hydrochar) by-products. The latter consists mainly of the inorganic fraction of the feedstock [4], with the potential for nutrient recovery and carbon sequestration.

Batch HTL has been extensively used for several biomass types, including microalgae, food waste, sludges, manure, lignocellulosic, etc. The product yields and product characteristics have been broadly studied and correlated to operating conditions [5]. However, it is not

* Corresponding author. Hangøvej 2, 8200, Aarhus, Denmark.
E-mail address: pbiller@bce.au.dk (P. Biller).

https://doi.org/10.1016/j.biombioe.2024.107166
Received 24 January 2024; Received in revised form 7 March 2024; Accepted 10 March 2024
Available online 18 March 2024

apparent that these results can be readily applied to continuous operation, which is preferable for industrial/commercial employment [6,7].

Nutrient recovery from the aqueous phase and hydrochar is a promising route to upcycle these by-products. Thus, there are numerous studies on the fractionation of inorganics in HTL products from batch reactions. Prior research reported that after batch HTL, less than 10% of K, Na, Cu, Zn, Cr, Ca, Mg and Al are commonly present in the biocrude [8]. Ca, Mg, Fe, and Al are more likely to migrate to the solid fraction, while K and Na to the aqueous fraction [9]. Nevertheless, this behaviour is influenced by the biomass composition, reaction conditions and extraction solvents. High temperatures (350–400 °C) have shown a higher share (20–30%) of heavy metals such as Cu, Ni and Pb to the biocrudes; while over 70% of P, Ca, Mg, Al, Fe, Mn, Zn, Cu, Cd, Cr, Ni, and Pb were in the solid fraction after HTL of animal manures and sludges [10]. In this way, separating nutrients from harmful elements is necessary for further utilisation of the hydrochar.

P has shown to be soluble in the aqueous phase at lower reaction temperatures (<200 °C) and tends to precipitate at higher reaction temperatures, depending on the feedstock composition and process conditions [11]. P from the hydrochar has been reclaimed as struvite after acid-leaching with ammonium contribution from the aqueous phase [12,13].

On the other hand, in continuous HTL, there is limited information on the hydrochar properties and composition, though there have been efforts to close the nutrient balances; however, challenges such as hydrochar separation hamper its full recovery [14]. Elliott et al. [15] attempted to close the P and N balances after continuous HTL of macroalgae at 350–364 °C. While no P was found in the aqueous and biocrude phases, N was primarily present in these two by-products. Remarkably, the solid separation mechanism could not recover most of the hydrochar; thus, the balances of these and other nutrients need to be further investigated under continuous operation. Ovsyannikova et al. [14] studied the nutrient distribution and P reclamation after HTL of sewage sludge and microalgae using a continuous pilot-scale reactor where the biocrude was separated from the hydrochar post-reaction by filtration. The obtained biocrude was still contaminated with solids and, thus, held a high content of inorganics such as Ca, P and Fe. These results show that in-line solids separation during continuous HTL could enhance the product's characteristics and facilitate post-processing [16].

Recently Wang et al. [17] compared the biocrude properties from batch and continuous reactions, demonstrating that the operating mode significantly influences the biocrude yields, energy content and composition. Nevertheless, no studies depict the differences between hydrochar from batch and continuous HTL nor the nutrient fractionation in continuous operation, which is a crucial step to achieving nutrient recovery and cleaner biocrude at industrial scales.

Therefore, the current research investigates the separation of inorganics from cattle manure using a separation mechanism incorporated in a semi-continuous reactor. The first objective was to assess the performance of in-line filtration within the continuous reactor as a function of reaction temperatures of 300, 325 and 350 °C to determine if temperature leads to additional precipitation of inorganics. The second objective was to comparatively evaluate the hydrochar characteristics and the inorganics fractionation into the HTL products from batch and continuous operation, to determine to which extent the batch product characteristics can be extrapolated to continuous operation and subsequent industrial processes.

2. Materials and methods

2.1. Materials

Approximately 200 L of cattle manure were collected during the winter and summer of 2022 from cattle stables of the Danish Cattle Research Centre. After collection, the material was dried on aluminium trays at 80 °C for about ten days. The manure collected in winter (~100 L) was milled using a CF158 grinder from EverTec, while the other half was milled using a Pulverisette 19 knife mill from Fritsch. Both batches were sieved using a 1 mm mesh, combined, and stored in an airtight container at ambient temperature for further use.

2.2. Batch experiments

The batch experiments were carried out in 20 mL stainless steel reactors using ~0.9 g of dried manure and 8.1 g of distilled water (10% solids). The reaction temperatures of 300, 325 and 350 °C were obtained in a Fluidized Temperature Sand Bath (FTBLL12 Accurate Thermal Systems, USA) at heating rates of approximately 56–66 °C/min.

After 20 min, the reaction was quenched in a water bath at ambient temperature. The gas content was quantified by weighing the reactors before and after opening. The rest of the reaction products were separated by centrifugation at 5000 rpm for 10 min. The resulting supernatant is the HTL aqueous phase, and it was stored at 5 °C until further analysis, while the biocrude/hydrochar matrix from the centrifuge tube and the reactor were dissolved in dichloromethane, VWR (DCM). The mixture was vacuum filtrated using VWR glass microfibre 413 filters, and the hydrochar filter cake was further washed with DCM and then dried at 105 °C overnight. The biocrude-DCM mixture was flushed under N_2 at ambient temperature until constant weight.

2.3. Continuous experiments

2.3.1. Reactor description

The continuous experiments were carried out in a custom-built plug flow reactor at 300, 325 and 350 °C. The feedstock was loaded as a slurry with 10% solids and 1% sodium carboxymethyl cellulose (CPKelco) as a pumpability enhancer. The tests were conducted at a constant flow rate of 45 ± 5 g/min, controlled by a hydraulically actuated diaphragm metering pump (MT8, Wanner Engineering). Seven heating tapes were used to reach the desired temperatures: four 940 W, two 1254 W and one 468 W. The pressure was kept at 180 ± 10 bar using a diaphragm back pressure regulator from Equilibar and monitored through six melt pressure transmitters (GPT300, Gamicos).

The reactor consists of over 13 m of Inconel 625 tubes and stainless-steel fittings with a 6 mm inner and 8 mm outer diameter with a total volume of ~700 mL. During operation, the reactor is taken to the desired reaction conditions using only demineralised water until stabilised at the temperature set point; subsequently, a pump directs water from a weight-controlled reservoir into the feeding tube (2 L capacity), which drives the biomass slurry into a heat exchanger employing a hydraulic piston. The heat exchanger consists of two 30 × 35 mm aluminium blocks with 8 mm tubes where the temperature is increased before taking it to the set point in the subsequent trim-heater section. The slurry then goes through approximately 5 m of reactor tubes and a solids-separation unit at constant reaction conditions. Finally, the filtrated slurry passes to the heat exchanger and a cooler unit where the temperature is lowered to about 70 °C. In the outlet, the gas volume is measured by a water displacement flowmeter (2 L XML, GN instruments), and the biocrude and aqueous phases are gravimetrically separated in a collection vessel. A schematic representation of the reactor is shown in Fig. 1.

2.3.2. Product separation

The solid separation unit consists of a cylindrical 316 L stainless-steel filter with a pore size of 20 μm enclosed within a 316 stainless-steel case with ~110 mL capacity.

During the stabilisation period of the system, the inlet and outlet valves of the filter unit are opened. Thus the filter is also rinsed with demineralised water at reaction conditions.

When the biomass slurry in the feeding tube is over, the reactor continues operating using demineralised water for at least one more

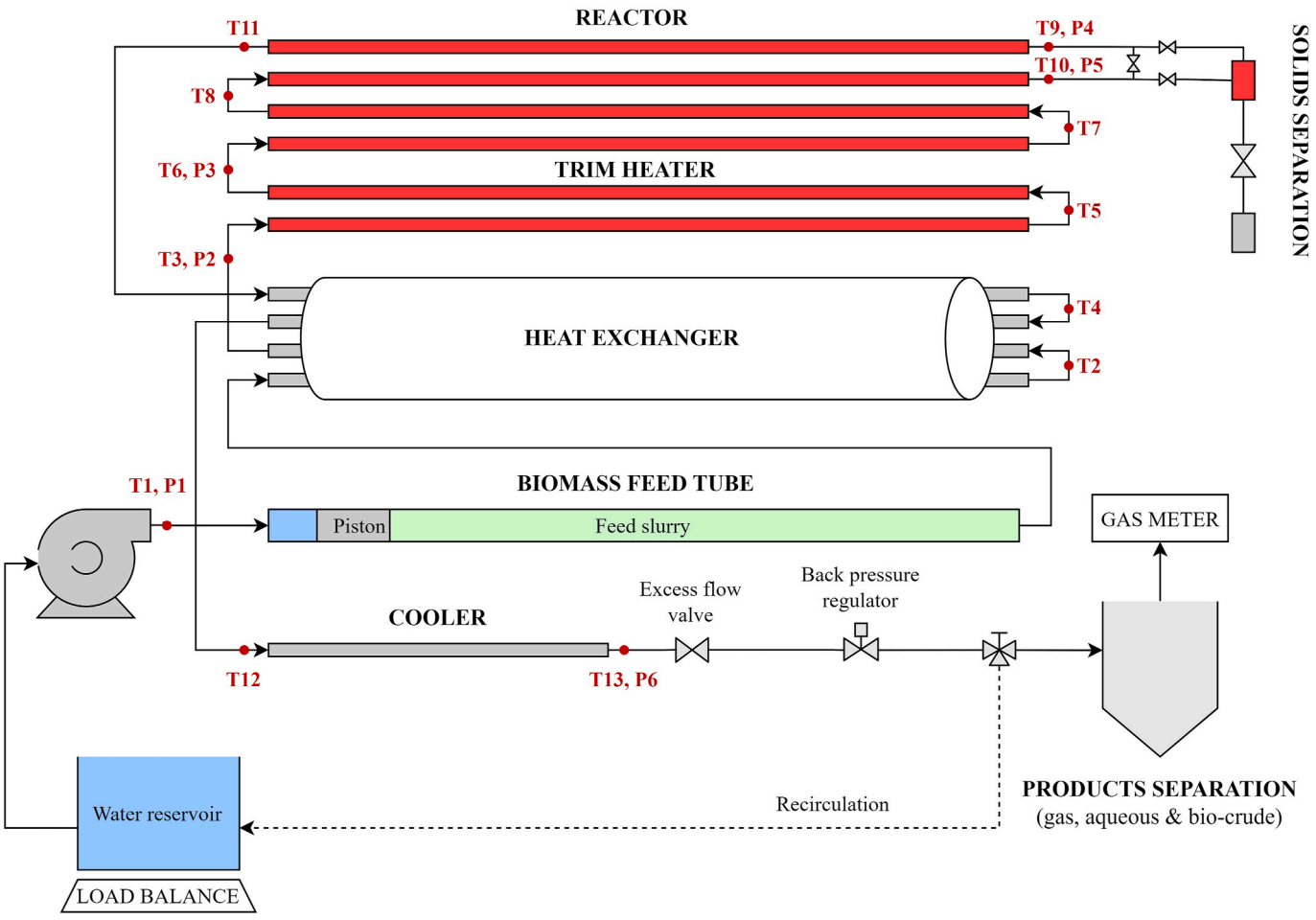

Fig. 1. Continuous HTL reactor schematic view. Ti (i=1:13) Is the data registered from the thermocouples at the indicated position. Pi (i=1:6) Is the data registered from the pressure sensors at the indicated position.

hour to ensure the biomass slurry has completely passed through the system.

Finally, the product collection vessel is removed, and the gas volume is no longer measured; the inlet and outlet valves of the filter unit are then closed, and the reactor continues operation with demineralised water until a temperature <100 °C is achieved. A total residence time of 11.6 ± 0.5 min was maintained during operation.

After cooling down, the solids separation unit is opened, and the hydrochar is collected and dried at 60 °C until constant weight. The aqueous and biocrude fractions were continuously collected during operation in the reactor outlet at ~70 °C and ambient pressure. After settling overnight, the aqueous phase is removed from collection vessel and the biocrude mass is measured.

In order to examine how effective the filter is in trapping the solids or whether there is char formation after the in-line filter, a portion of the biocrude was dissolved in DCM and vacuum filtrated using VWR glass microfibre 413 filters. The retained solids were re-suspended in DCM and stirred for at least 10 min after which they were filtered again. The last step was repeated one more time and the final filterable solids, hereafter referred to as extracted hydrochar, were dried at 105 °C. The DCM was separated from the biocrude, hereafter referred to as extracted biocrude, using a rotary evaporator (IKA RV 10 auto) at 40 °C and pressures between 730 mbar and atmospheric.

2.3.3. Yields calculation

For both reaction types, the gas composition was assumed as 100% CO_2. The ideal gas equation (Eq. 1) at standard conditions was used to calculate the mass of CO_2. Eq. (2). was used to calculate the hydrochar, biocrude and gas yields.

$$M_G[g] = \frac{R * T * MW_{CO_2}}{P * V} \quad \text{(Eq. 1)}$$

$$Y_i[\%] = \frac{M_i}{M_S} * 100 \quad \text{(Eq. 2)}$$

Where M_G is the mass of gas calculated using the ideal gas law and the molecular weight of CO_2 (MW_{CO_2}), R is the ideal gas constant (0.082 $\frac{atm*L}{K*mol}$), T is the temperature Y_i is the yield of product i (G: gas, B: biocrude or H: hydrochar), M_i is the mass (dry basis) of product i, and M_S is the mass of manure added to the feedstock slurry.

Finally, the liquid yield (Y_L) was calculated by difference using Eq. (3).

$$Y_L[\%] = 100 - Y_B - Y_H - Y_G \quad \text{(Eq. 3)}$$

2.4. Summary of operating conditions in batch and continuous HTL

To summarize the details given in the previous sections, Table 1 presents the operational parameters used for the batch and continuous HTL experiments.

While the use of DCM is inherent to product separation in batch reactions due to the resulting products mix where all the char and all the biocrude are mixed, the absence of DCM in continuous operation is due to the methodology implemented in this mode. The in-line solids separation device installed in the continuous reactor allowed the separation of a biocrude-free char. Tests on this char showed that DCM extractions,

Table 1
Operating conditions for batch and continuous HTL experiments of cattle manure.

Parameter	Unit	Batch	Continuous
Number of replicates	–	9	2
Feedstock loading	%[a]	10	10
Pumpability enhancer (CMC)	%[a]	–	1
Reaction temperature	°C	300 325 350	300 325 350
Pressure	bar	85.9 (Autogenous) 120.5 (Autogenous) 165.3 (Autogenous)	185
Time at reaction conditions	min	15	4.4
Flow rate	g/min	–	46
Char separation		Char/biocrude mix dissolved in DCM and vacuum filtered	i. ~74% of char filtered at reaction conditions. ii. ~26% of char resulted in biocrude, it was dissolved in DCM and vacuum-filtered

Notes: The numbers correspond to average values through the experiments. [a]of total slurry.

under the same conditions as in batch reactions, only allowed the recovery of ~0.7% biocrude; thus, DCM extraction was omitted for these samples. The continuous biocrude was subjected to DCM extractions to examine the effectiveness of the filter element in removing char and char formation post-filtration.

2.5. Analytical methods

The identification label of the products is "RTP", where R is the reaction type (C for continuous and B for Batch or E for the extracted hydrochar and solids-free biocrude after continuous reactions) used to obtain the products P (B for biocrude, H for hydrochar, A for aqueous and G for gas), at the operational temperature T (300, 325 or 350 °C). For example, the code C300H corresponds to the hydrochar product derived from a continuous reaction at 300 °C, while the code E325B corresponds to the biocrude obtained from a continuous reaction at 325 °C after it has been dissolved in DCM and filtered.

The ash content of the manure, the hydrochars and biocrudes from the semi-continuous reaction were determined by igniting the samples at 550 °C for 3 h (heating rate of 5 °C/min) using a Nabertherm muffle furnace. The procedure was adapted from ISO 18122:2015.

Due to the limited amount of hydrochars and biocrudes obtained from batch reactions, the ash content was determined by thermogravimetric analysis (TGA) using a Mettler Toledo TGA/DSC 3+.

The samples were heated under a N_2 stream of 50 mL/min to 105 °C and a heating rate of 10 °C/min, held for 20 min at 105 °C and then further heated to 550 °C at the same heating rate. The temperature was maintained at 550 °C for 20 min. Finally, the N_2 stream was switched to air to ignite the samples during 60 min, adapted from Refs. [18,19].

To examine the volatile matter and fixed carbon (Eqs. (4) and (5)) in the samples by TGA, the following program was employed using a N2 stream of 50 mL/min.

Segment 1: Ramp from 50 to 105 °C at 20 °C/min
Segment 2: Isotherm at 105 °C for 15 min
Segment 3: Ramp from 105 °C to 900 °C at 20 °C/min
Segment 4: Isotherm at 900 °C for 15 min

The batch hydrochar samples were oven-dried at 105 °C for 24 h; thus, the moisture content obtained via TGA was consistently <0.7% and was assumed as negligible.

$$VM[\%db] = 100\frac{mass\ residue\ end\ of\ segment\ 2 - mass\ residue\ end\ of\ segment\ 4}{Initial\ mass\ dried\ at\ 105°C} \quad \text{(Eq. 4)}$$

$$FC[\%\ db] = 100\% - VM[\%\ db] - Ash[\%\ db] \quad \text{(Eq. 5)}$$

The total carbon (TC) and total nitrogen (TN) analyses were performed using a Formacs HT TOC/TN analyser (Skalar, The Netherlands).

The major elements C, H, N and S in the feedstock, biocrudes and hydrochars were quantified using a vario MACRO cube elemental analyser (Elementar, Germany). The O content was calculated by difference using Eq. (6).

$$O[\%] = 100 - C - H - N - S - A \quad \text{(Eq. 6)}$$

The higher heating values of the feedstock, biocrudes and hydrochars were calculated on the basis of the elemental analysis using Eq. (7), suggested by Channiwala and Parikh [20].

$$HHV\left[\frac{MJ}{kg}\right] = 0.3491C + 1.1783H + 0.1005S - 0.1034O - 0.0151N - 0.0211A \quad \text{(Eq. 7)}$$

where C, H, N, S and A in both equations are the samples' carbon, hydrogen, nitrogen, sulphur, and ash content, respectively, expressed as mass percentages on a dry basis.

On the other hand, the inorganics P, Ca, Mg, Na, K, and Fe were determined in all samples by inductively coupled plasma optical emission spectrometry (ICP-OES) using a PerkinElmer Optima 4300 ICP-OES. Before analysis, the samples were digested in nitric acid (Merck, 65%) in an Anton Paar Multiwave 3000 microwave.

All the analyses were conducted in triplicates for the feedstock and duplicates for the HTL products. The results are reported on a dry basis unless otherwise stated. The results in all tables and figures are expressed as the average ± the standard deviation. In all cases referring to process variability. The elemental balances were established based on the element content in the feedstock, the HTL products and their yields, and the volume of the aqueous phase.

The particle size distribution of the feedstock and hydrochars were determined by laser diffraction using a Malvern Mastersizer 2000 with a Hydro 2000MU sample dispersion unit. The samples were suspended and continuously stirred in demineralised water. A portion of the suspension was then added to the sample dispersion unit in approximately 1 L of previously sonicated demineralised water during continuous flow through the equipment. The share of particles in %v/v between 0.02 and 2000 μm was then measured by two light sources (red light: helium neon laser, and blue light: solid state light source). The results are shown as the average of five measurements.

Py-GC-MS analyses were performed using a multi-shot pyrolyzer (EGA/Py-3030D, Frontier Laboratories Ltd., Fukushima, Japan) interfaced to a 7890 B Agilent HP gas chromatograph (GC) coupled with a 5977 B Agilent HP quadrupole mass spectrometer (MS) (Agilent Technologies, Palo Alto, USA). The samples (6 ± 0.1 mg) were pyrolyzed at 600 °C for 1 min with helium as carrier gas (1 mL/min), and the Py-GC interface was kept at 280 °C. The GC injector was operated in split mode with a split ratio of 1:20 and a temperature set to 280 °C. The column oven temperature was programmed as follows: the initial temperature was maintained at 50 °C for 2 min, increased to 280 °C at 10 °C/min, and maintained at 280 °C for 8 min. The MS was operated in electron impact ionization mode (70eV, scanning 10–600 m/z) with transfer line temperature 250 °C, ion source temperature 230 °C and quadrupole temperature 150 °C. The data were collected and processed by Agilent MSD ChemStation software using NIST reference library for mass spectral identification or comparison to published literature data. Py-GC-MS analyses were performed in triplicate with procedural blanks before

each set of analysis.

3. Results and discussion

3.1. Feedstock characteristics

The proximate and ultimate analysis and the inorganic composition of the manure are shown in Table 2.

The ash content of the manure was 20.1 %, which is within the range of reported values in other studies (10.0–34.9%) [21–24]. As an indicator of inorganic matter, variations in the ash content of different manure samples may be related to the presence of sand, animal hair and minerals resulting from the animal feed and handling and storage.

In line with the high ash content, the feedstock is rich in K, Ca, Na, Mg and P (7014–25250 mg/kg), moreover, a relatively high N content (2.59 %) increases the nutrient potential recovery of manure. The C content was comparable to other cattle manure samples found in literature [25].

3.2. Products yields

The difference in product yields after continuous and batch reactions can be observed in Fig. 2. In general, the biocrude yields in batch and continuous reactions are in the same range of 24–27%, as documented also by Liu et al. [26], showing a trend to increase slightly with increasing reaction temperature. Remarkably, at 350 °C the biocrude yields of the continuous reaction were up to 8% higher than in batch reactions, reaching ~34%. However, the biocrude yield in continuous reactions drops to 21–30% after the separation of the filterable solids, which allows the following hypotheses: (i) the in-line filter does not separate all the char as a result of smaller particles passing through the filter pores, (ii) there is char formation after the in-line filter, and (iii) due to the instability of the biocrude, solids formation occurs during sample storage. In fact, a combination of the aforementioned factors is highly likely, they will be discussed further in sections 3.4 and 3.6.

Regarding the hydrochar, in batch reactions there is a yield reduction from 24% at 300 °C to 17% at 350 °C. In contrast, lower solids yields were observed in continuous HTL where the hydrochar filtered at reaction conditions was between 11 and 14%, while the total hydrochar yield (adding up to the extracted char post-reaction) were 19.2, 15.5 and 15.0% at 300, 325 and 350 °C, respectively. Other studies on batch HTL of cattle manure have reported a wide range of biocrude and hydrochar yields, ranging from 19 to 39% and 20–45% [9,23].

Table 2
Cattle manure characteristics.

Proximate analysis			
Volatiles, %	61.9	±	0.4
Fixed carbon, %	16.4	±	0.3
Ash, %	20.1	±	0.4
Ultimate analysis			
C, %	42.9	±	0.0
H, %	6.1	±	0.0
N, %	2.6	±	0.0
S, %	0.6	±	0.0
O[a], %	27.8	±	0.4
HHV, MJ/kg	18.8	±	0.1
Inorganic content, mg/kg			
P	7014	±	532
Ca	18368	±	1609
Mg	7787	±	540
Na	8567	±	296
K	25250	±	438
Fe	749.1	±	73.7

[a] Calculated by difference.

These differences can be attributed to the different reactor types, the in-line solids separation unit in the continuous reactor and the solvent separation method used for solids/biocrude recovery. Solids separation at reaction conditions and relatively low residence time may prevent the re-polymerization of reaction intermediates [24]; this is also reflected in the lower carbon recovery of the continuous hydrochars compared to the batch hydrochars (Fig. 3) and the low yields (3.6–5.5%) of the continuous extracted hydrochars. Furthermore, the mixing effect of the continuous flow may enhance heat and mass transfer allowing a more extensive decomposition of the biomass. A similar trend of lower hydrochar yields in continuous HTL of lignocellulosics was also described elsewhere [17].

It is worth mentioning that the CMC in its salt form could have a catalytic effect on the HTL process. The use of alkali catalysts in HTL research has shown reduced char formation and favoured biocrude production [26–28], with several studies agreeing that K-based catalysts and carbonates have a stronger effect than the corresponding Na and hydroxide forms [29].

Furthermore, the CMC present in continuous experiments may serve as an additional carbon source, expected to behave in a similar way to cellulose. Prior screening studies performed in batch reactions showed that the addition of 1% CMC to the slurry did not have a measurable impact on the product yields or the elemental composition of the resulting biocrudes and hydrochars. Therefore, we expect the effect of CMC to be minimal when comparing batch to continuous.

On the other hand, the gas yields ranged from 21 to 35 % in batch reactions, being larger at higher temperatures, while they showed less variation in continuous operation (29–31%). For simplicity reasons, it was assumed that the gas was composed of 100 % CO_2, which is an accurate assumption given a deviation of only ±1% in the gas yields compared to the average HTL gas composition (92% CO_2, 6.8% CO, 0.7% H_2 and 0.5% CH_4) calculated after a literature survey for HTL of cattle manure [23,30,31].

3.3. Carbon and nitrogen balances

The C and N recoveries in the HTL products (Fig. 3) were calculated considering the products yields, TC and TN of the aqueous fraction and the CHNS content of the feedstock, hydrochar and biocrude samples, and the aforementioned assumption for the gas composition.

In both batch and continuous reactions 29–44% of the C was recovered in the biocrude, Continuous extracted biocrudes at 300 °C (E300B) showed less carbon recovery than their batch counterpart B300B, while E350B displayed the highest C recovery. Regarding N, it was found predominantly in the aqueous phase for both reactions, but there was a higher partitioning in continuous HTL, where it corresponded to 49–56% of the total N. The composition of HTL AP of cattle manure has been reported to have a high content of N-heterocycles and aminophenols as a result of organic acids reacting with ammonia [23]. Other studies reported over half of the N in chicken and swine manures was present mainly as NH_4^+ in the HTL AP, the study suggested that organic N is further degraded to inorganic N with increasing reaction temperature [32].

Concerning the hydrochars, batch reactions exhibit higher C recovery, 16–25 %, decreasing with increasing reaction temperature. Comparatively, C recovery in continuous hydrochars was between 4 and 8% for the char separated at reaction conditions; such a low recovery was expected given the low C contents (Table 3) in agreement with [33]; the chars extracted post reaction, had a C recovery of 5–8%, due to their low mass yields (3.6–5.5%). The combined C recovery in continuous hydrochar accounted for 10% at 350 °C to 16% at 300 °C. A similar behavior was observed for N.

Prior research on hydrothermal conversion of biomass agrees that the term hydrochar may encompass two kinds of solids: (i) primary char which is the result of solid-solid conversion of the biomass after

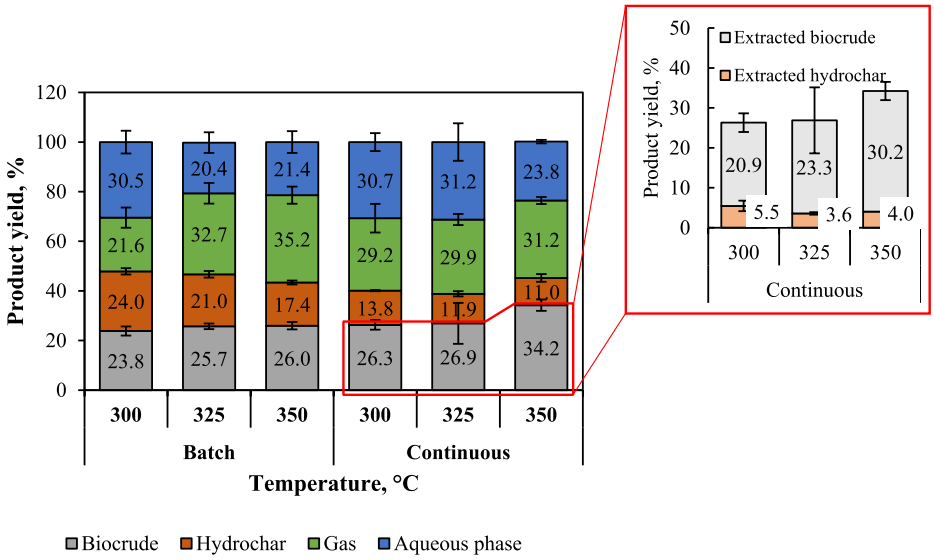

Fig. 2. HTL product yields from cattle manure at 300, 325 and 350 °C in batch and continuous reactions. Error bars: standard deviation with n = 9 for batch and n = 2 for continuous. The data callout represents the extracted hydrochar and extracted biocrude yields from the continuous experiments with respect to the dry feedstock.

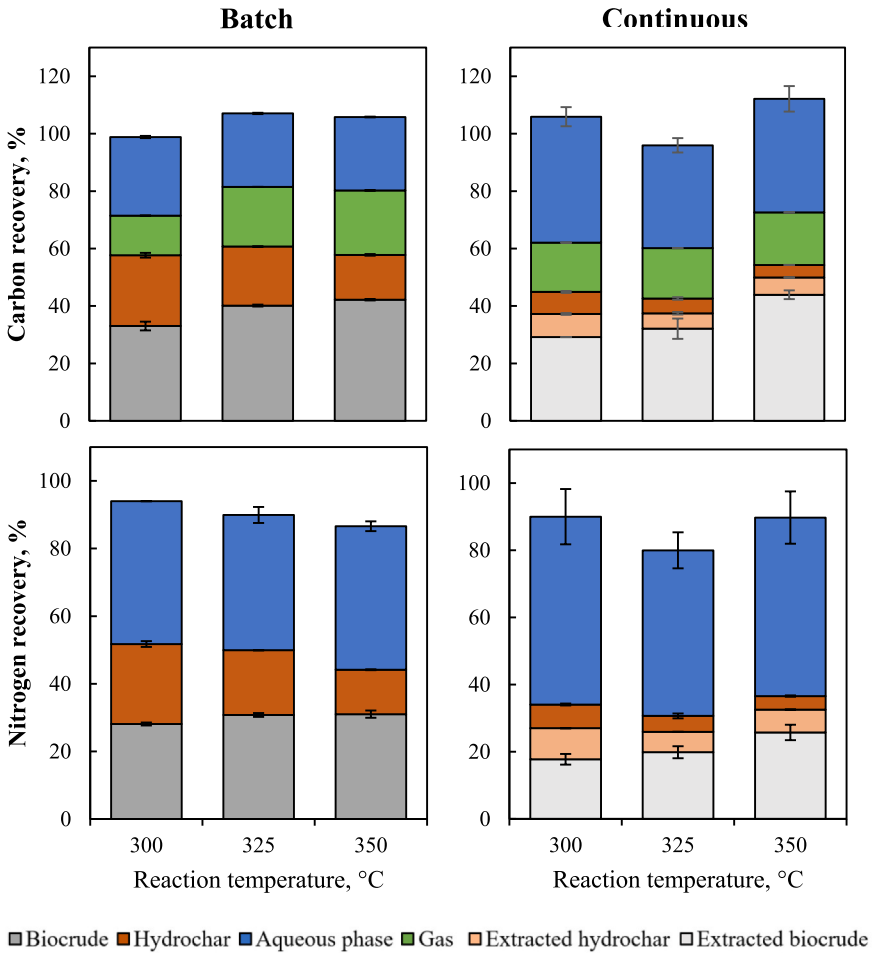

Fig. 3. C and N balances in batch and continuous HTL reactions at 300, 325 and 350 °C.

Table 3
Proximate and ultimate analysis and higher heating value of biocrudes and hydrochars from batch and continuous reactions at 300, 325 and 350 °C.

Sample			Volatiles, %	Fixed carbon, %	Ash, %	C, %	H, %	N, %	S, %	O, %	HHV, MJ/kg
Manure			65.9 ± 0.5	14 ± 0.7	20.1 ± 0.4	42.9 ± 0	6.1 ± 0	2.6 ± 0	0.6 ± 0	27.8 ± 0.4	18.8 ± 0.1
Hydrochar	Batch	**B300H**	36.7 ± 1.9	24.8 ± 3	38.5 ± 2.3	43.9 ± 1.5	3.5 ± 0.1	2.5 ± 0.1	0.8 ± 0	10.7 ± 2.7	17.6 ± 0.6
		B325H	33.9 ± 1.2	25.1 ± 2.9	41 ± 2.6	42 ± 0	3.2 ± 0.1	2.4 ± 0	< LoD	11.4 ± 2.6	16.3 ± 0.3
		B350H	27.2 ± 2.8	24.2 ± 3	48.7 ± 0.9	38.4 ± 0.7	2.7 ± 0	2 ± 0	< LoD	8.2 ± 1.2	14.7 ± 0.3
	Continuous	**C300H**	24.5 ± 0.1	8.6 ± 1.2	66.9 ± 1.2	26 ± 1.1	1.8 ± 0	1.3 ± 0.1	< LoD	4 ± 1.6	9.3 ± 0.4
		C325H	21.4 ± 0.8	5.3 ± 3.4	73.3 ± 3.3	20.1 ± 1.5	1.4 ± 0.1	1 ± 0.2	< LoD	4.1 ± 3.7	6.7 ± 0.7
		C350H	18.7 ± 1.7	3.2 ± 3.2	78.1 ± 2.7	18.4 ± 0.1	1.2 ± 0	1 ± 0	< LoD	1.3 ± 2.7	6.1 ± 0.3
		E300H	49.9 ± 0.8	49.6 ± 0.9	0.5 ± 0.6	68.8 ± 0.2	5.5 ± 0.3	4.4 ± 0	< LoD	20.8 ± 0.7	28.3 ± 0.4
		E325H	47.2 ± 0.2	51.5 ± 0.9	1.3 ± 0.8	69.5 ± 0.5	5.6 ± 0.1	4.2 ± 0	< LoD	19.4 ± 1	28.8 ± 0.3
		E350H	45.9 ± 0.3	52.3 ± 0.3	1.8 ± 0.1	69.6 ± 0.4	5.5 ± 0.1	4 ± 0.1	< LoD	19.2 ± 0.4	28.6 ± 0.2
Biocrude	Batch	**B300B**	75.9 ± 0.9	10.1 ± 4.2	13.9 ± 4.1	59.4 ± 2.8	6.6 ± 1	3.1 ± 0	< LoD	17 ± 5	26.4 ± 1.6
		B325B	77.1 ± 1.9	13.7 ± 2.2	9.1 ± 1.1	66.9 ± 0.5	7.3 ± 0.1	3.1 ± 0.1	< LoD	13.6 ± 1.2	30.3 ± 0.2
		B350B	75.9 ± 0.6	16 ± 2.4	8.2 ± 2.3	69.7 ± 0.5	7.6 ± 0.1	3.1 ± 0.1	< LoD	11.5 ± 2.4	31.9 ± 0.3
	Continuous	**C300B**	69 ± 1.8	30.6 ± 1.8	0.3 ± 0.2	61.2 ± 5.8	8 ± 0.5	2.9 ± 0.2	< LoD	27.6 ± 5.8	27.9 ± 2.2
		C325B	60.8 ± 8.1	38.8 ± 8.1	0.4 ± 0.1	57.3 ± 2.5	7.2 ± 0.6	2.6 ± 0.2	< LoD	32.5 ± 2.5	25 ± 1.1
		C350B	63.7 ± 11.8	36 ± 11.8	0.3 ± 0.1	69.8 ± 6.4	8.4 ± 0.3	2.9 ± 0.1	< LoD	18.6 ± 6.4	32.3 ± 2.4
		E300B	81.6 ± 0.4	18.4 ± 0.4	0 ± 0	65.1 ± 2.1	7.6 ± 0.2	2.2 ± 0.2	< LoD	25.1 ± 2.1	29.1 ± 0.8
		E325B	81.7 ± 0.3	18.3 ± 0.3	0 ± 0	64.1 ± 0.7	7.2 ± 0.2	2.4 ± 0.04	< LoD	26.4 ± 0.7	28 ± 0.4
		E350B	80.4 ± 0.7	19.5 ± 0.7	0.1 ± 0.1	67.6 ± 1.5	7.3 ± 0.2	2.6 ± 0.07	< LoD	22.4 ± 1.5	29.9 ± 0.6

All results are presented on a dry basis. * Calculated by difference.

undergoing hydrolysis, dehydration, decarboxylation and aromatization reactions, and (ii) secondary char, commonly defined as the product of the polymerization/condensation of reaction intermediates released during reaction from the feedstock into the liquid phase [34]. Accordingly, the extracted hydrochar from the biocrude in after continuous HTL can be catalogued as secondary char. Reports suggest that the C content in secondary char significantly higher carbon content than the primary char [35], as it confirmed in Table 3.

3.4. Ultimate, proximate analysis and thermal stability

Table 3 presents the elemental composition, ash content and estimated higher heating values (HHV) of the hydrochars and biocrudes. All measurements are reported on a dry basis. The moisture content of the hydrochar trapped in the filter during continuous HTL was measured at 81.0 ± 2.3%.

The ash content of the hydrochars from continuous reactions was remarkably higher (67–78%) than for batch reactions (38–49%). In both cases accompanied by a reduction in the C content with increasing reaction temperature. The increment in the ash content for both reactions may be the result of a more extensive conversion of organic compounds into other product fractions as well as inorganics precipitation when the reaction condition approach the critical point of water [36].

The continuous operation herein employed involves flushing the reactor with a pure demineralised water stream at reaction temperature at the end of the experiment to ensure that most of the biomass is converted and does not remain stagnant within the reactor (preventing clogging and plugging). Therefore, the water may have washed away the biocrude from the char entrapped within the filter element, given the low biocrude viscosity at reaction conditions. Likewise, the water flushing may have also enhanced the removal of water-soluble elements such as Na and K.

Notable contrasts were also observed for batch and continuous biocrudes. After continuous operation, the ash content of the biocrudes was less than 1%, while batch biocrudes had up to 14% ash; nevertheless, their HHVs were in the same range due to the higher oxygen estimation in continuous biocrudes.

Similarly, the ash content of continuous biocrudes was reported to be lower than for batch biocrudes after HTL of black liquor (6.9 vs 11.7 %) [17]. Interestingly, no in-line solids separation was used, thus the reaction type alone contributed to an improved inorganics separation although to a lower extent.

Regarding the aforementioned hypothesis (ii. There is char formation after the in-line filter), possibly the ash (inorganics) removal mid-reaction in continuous HTL limited the repolymerization of reaction intermediates, reducing the secondary char formation and lowering carbon recovery in both the primary and secondary chars, this may indicate a catalytic effect of some inorganics on the char formation that is observed in batch HTL but not in continuous HTL with in-line solids separation.

The van Krevelen diagram in Fig. 4 highlights the similarities between the batch hydrochars and the continuous secondary hydrochars in terms of H/C and O/C which contrast with the lower H/C and O/C ratios of the primary char from continuous reactions, indicating a higher degree of dehydration. Nevertheless, the H/C ratio shows little variation: for biocrudes it ranged between 1.3 and 1.6, being higher for the continuous biocrudes, in alignment with other studies [23,25], while for hydrochars ranged between 0.8 and 1.0, being slightly lower for the continuous hydrochars. In all cases, the highest temperature contributed to the largest reduction of H/C and O/C.

Fig. 5 shows the thermal degradation behaviour of the raw manure

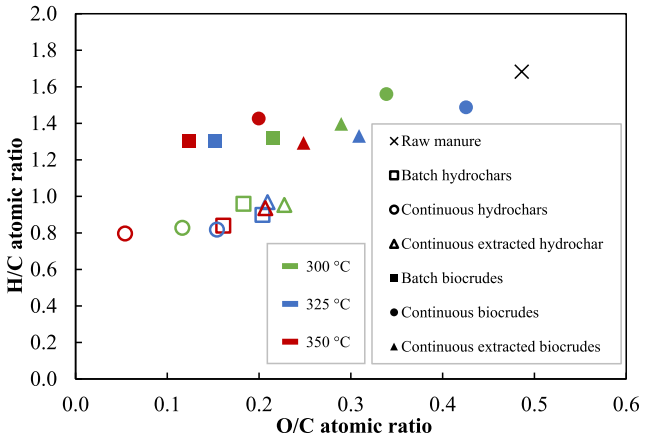

Fig. 4. Van Krevelen diagram of the hydrochars and biocrudes obtained from batch and continuous HTL at 300, 325 and 350 °C.

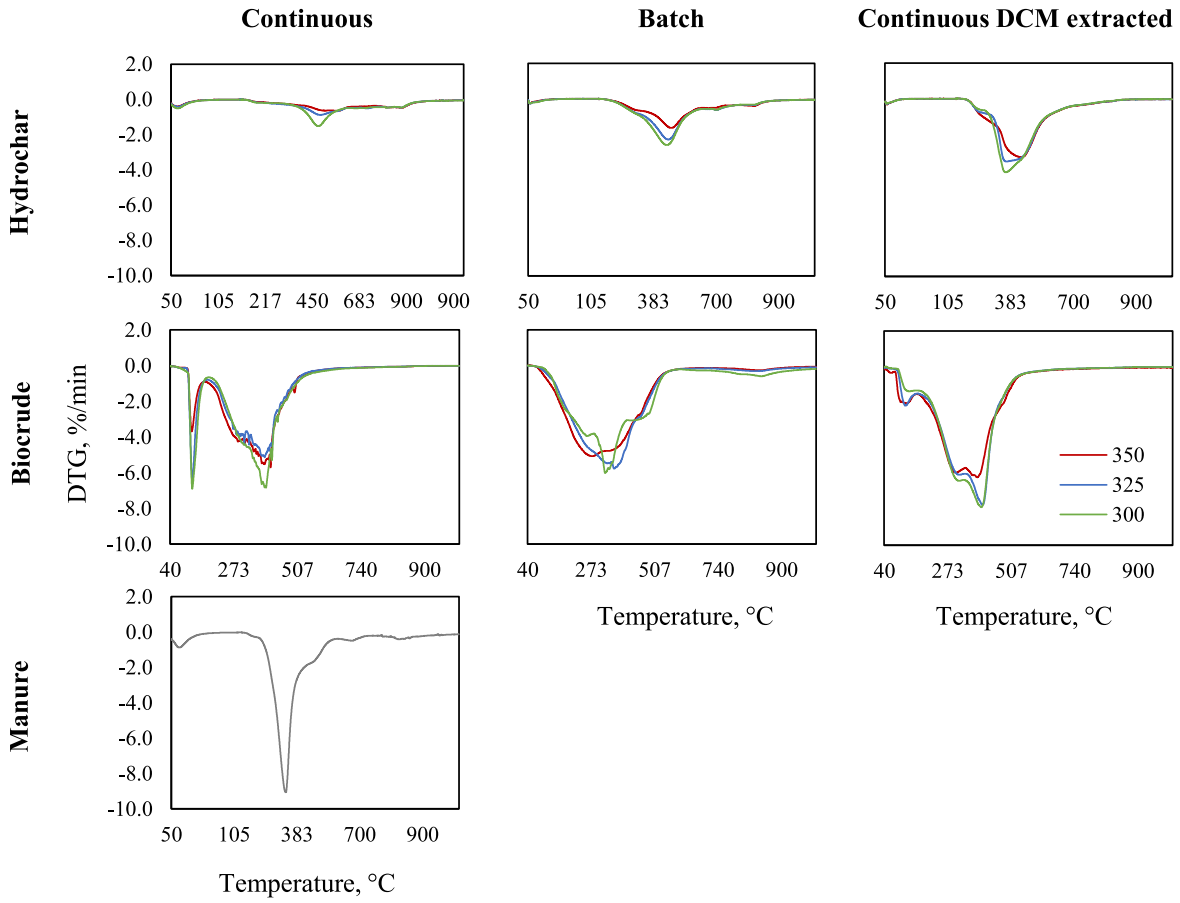

Fig. 5. DTG profiles of cattle manure and the produced biocrudes and hydrochars from batch and continuous HTL at 300, 325 and 350 °C.

and compares the thermal degradation characteristics of the hydrochars and biocrudes obtained by batch and continuous HTL.

The continuous biocrudes had a rapid mass loss between 105 and 145 °C where about 10% of the mass was volatilized, revealing a higher presence of low boiling point compounds. In contrast the mass loss for batch biocrudes started at about 135 °C at a much lower rate. This may be an indication of the loss of volatile matter during the DCM evaporation phase for batch biocrudes. Wang et al. [17] found that after HTL of pinewood and cornstalk, continuous biocrudes had over 10% more of highly volatile furans compared to batch biocrudes. This finding was attributed to the lower residence time in continuous HTL that could prevent to the repolymerization of furans into larger molecules or into char. Indeed, furans derivatives have been detected in hydrochars and furan intermediates in biocrudes from batch HTL of cellulose rich feedstocks [37]. In fact, several proposed HTL reaction pathways include furans as hydrochar precursors [38].

After the removal of secondary char from the continuous biocrudes, the resulting extracted biocrude showed less volatile matter loss in the lower temperature range but a larger peak in the main degradation zone. This is consistent with the DCM effect observed for batch biocrudes. And suggests that while DCM extraction decreases the share of low boiling point compounds, the secondary char extraction was responsible for around half of the fixed carbon content of the continuous biocrudes, as noted in Table 3.

In broad terms the thermal degradation profile of the solids exhibited three stages: an initial slight but steady mass loss stage where under 5% of the mass was volatilized, the main degradation zone evidenced in the sharp DTG peaks, at distinct temperatures for each char type, followed by another slight mass loss stage, as evidenced in Fig. 5. The continuous primary char showed more stability up to 360 °C where the effect of the reaction temperature was evident on both the rate and amount of volatilized matter, the main degradation zone occurred between 415 and 500 °C, peaking at 470 °C, in alignment with a high ash content. On the other hand, the thermal degradation profile for batch hydrochars showed an earlier initial stage at around 280 °C, while the main degradation stage was 330–500 °C, with peaks at 445 °C for B300H and B325H and 465 °C for B350H.

For the continuous secondary chars, the initial mass loss stage occurred at ~295 °C and the main degradation was within 300–550 °C. The hydrochars obtained from HTL at 350 °C showed a higher thermal stability than the ones from 325 and 300 °C, which behaved similarly. These results are consistent with [18] who examined the thermal degradation profiles of paunch waste hydrochars after hydrothermal conversion. The more volatile nature of secondary char is also accompanied by a high content of fixed carbon ranging from 49.6 to 52.3, increasing with reaction temperature, this indicates that over half of the re-polymerization products that compose secondary char are thermally stable C compounds, in agreement with [35]. Moreover, the thermal stability of the primary char obtained from continuous HTL of cattle manure lies primarily on its high ash content.

3.5. *Nutrient fractionation*

The distribution of nutrients from cattle manure was studied in the HTL products, assuming that there is no P, Ca, Mg, Na, K and Fe partitioning into the gas phase, their balances were established and reported in Fig. 6.

Both reaction types induced the quasi-total recovery of P in the hydrochars, and to some extent Ca and Mg. It is accepted that the metal (Ca, Mg, Fe, Al) phosphate precipitates is the main mechanism of P transfer to the solid product under hydrothermal conditions [39,40]. The Ca/P and Mg/P molar ratios of the hydrochars did not show notable

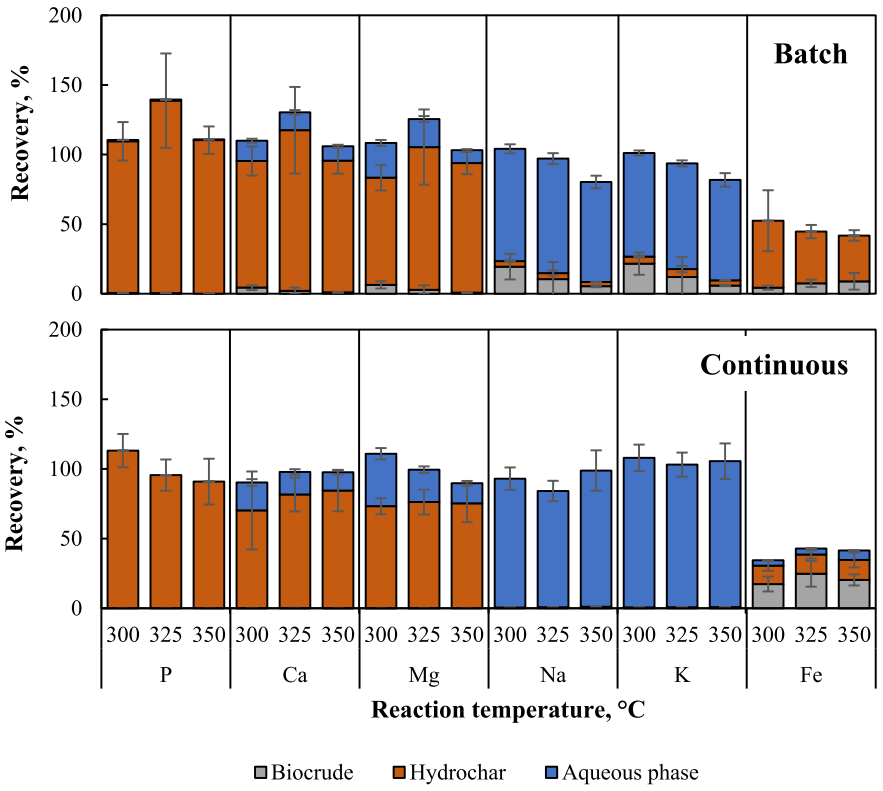

Fig. 6. Nutrients balances in batch and continuous HTL reactions at 300, 325 and 350 °C.

variations between batch and continuous HTL, or at the different reaction temperatures.

Previous studies on the biomass ash solubility and composition showed that P, Ca and Mg tend to be insoluble post combustion and are most likely converted to phosphates, oxalates, carbonates, CaO and other Ca species [41], correspondingly, previous XRD analyses of HTL hydrochars revealed the presence of several minerals including hydroxyapatite, nesquehonite, magnesite, monetite and tricalcium phosphate [37].

In accordance with other studies, alkali metals predominantly dissolve in the aqueous fraction in subcritical conditions. In batch reactions however, up to 20% of Na and K were detected in B300B and up to 5% in B350B. In contrast, <1% were detected in continuous biocrudes. A study based on model salt compounds suggested that Na and K are possibly present in the HTL aqueous phase as carbonate, sulphate or nitrate compounds [42], however, in this study the inorganic C content of the HTL aqueous phase in all the samples was very low and the raw manure had intrinsically a low S content. On the other hand, the ammonium content of the aqueous phase samples was between 30 and 50 % of the total N, suggesting the presence of Na and K as nitrates [23].

The Fe recovery was low for both reactions but there were major differences in the Fe content of biocrudes. Most Fe in continuous reactions was found in the biocrude. This may be due to a few reasons. First, it has been reported that the solvent to extract biocrude may also influence its heavy metal content, for instance, solvents such as DCM generated biocrudes with higher Fe than less polar solvents [43]. Even though there was no solvent used to separate primary char during the continuous reactions, the aqueous phase at reaction conditions could be responsible for this behaviour; however, this hypothesis may seem counterintuitive given the drop in polarity of water when approaching the critical point.

Secondly, the different materials employed in the reactors. The batch reactions were carried out in stainless steel vessels, while the continuous reactor was constituted of three materials: inconel 625 tubes, 316 L stainless steel fittings and 316 stainless steel filtercase. Nevertheless, the low overall Fe recovery does not allow to make any firm conclusions.

3.6. Particle size distribution of the chars

Fig. 7. Shows the particle size distribution of batch and continuous hydrochars at three process temperatures. Particle precipitation is controlled by temperature, type and content of salts in the feedstock and mixing throughout the reaction, while their size is determined by the prevalence of either nucleation or growth mechanisms, which in turn are influenced by the supersaturation of the mixture. Low levels of supersaturation tend to favour particle growth, because of the lower precipitation rate, then larger particles would form [44]. In the same way, dilute solutions may also decrease supersaturation and favour the

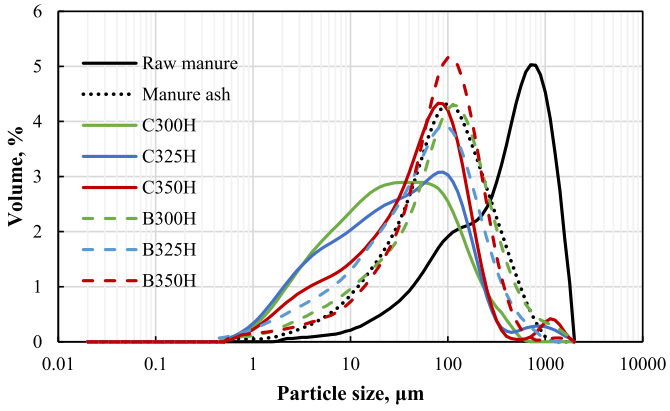

Fig. 7. Particle size distribution of hydrochars obtained from continuous and batch reactions at 300, 325 and 350 °C.

Table 4
Key percentiles of the particles' diameters for feedstock and hydrochars from batch and continuous HTL at 300, 325 and 350 °C.

Sample	d (0.1), μm	d (0.5), μm	d (0.9), μm
Raw manure	54.9	453.1	1228.3
Manure ash	15.9	93.6	343.1
B300H	11.0	95.2	349.9
B325H	6.5	63.3	243.6
B350H	14.9	89.2	250.3
C300H	3.8	28.0	149.9
C325H	3.5	34.0	175.0
C350H	5.3	53.6	181.0

formation of larger particles, thus the water rinsing at the end of the continuous reactions could have contributed to increasing the particle size, however, the mean diameters in batch hydrochars were consistently larger than for continuous chars, Table 4. A possible explanation could be the higher relative supersaturation within the filter element in the continuous reactor, which had a relatively lower capacity to capture solids than the batch reactor.

Regarding the reaction temperature, continuous reactions show an apparent char mean diameter increase with reaction temperature which may be related to an enhanced solubility at higher temperatures. However, these observations should be regarded as a preliminary screening of char's particle formation, and more/deeper investigation is needed to support/disprove these hypotheses.

Even though salt precipitation is more commonly studied at supercritical conditions with model compounds, it was shown that subcritical conditions also favoured the recovery in the solid phase of salt-forming elements such as Mg, Ca, and Fe, according to the char's inorganic composition.

Additionally, the in-line solid separation hinders further interaction between the precipitated solids and the liquid products during the cooling of the products, thus solid formation by particle growth may be inhibited but nucleation mechanisms may still be active and contribute to the so-called secondary char formation, as mentioned in section 3.4.

The hydrochar from batch reactions behaved more like a colloidal suspension when added to the water prior to analysis. This behaviour may indicate a key difference in terms of hydrophobicity and thus the non-polar nature of the batch hydrochars.

3.7. Hydrochar's organic composition

Fig. 8 shows the pyrolysis products of the manure, batch hydrochars and continuous primary chars obtained by Py-GC-MS. The results are expressed as area percent; therefore, they do not express the concentration of the different functional groups but give an indication of the variations between samples.

The raw manure is characterized by releasing a high content of oxygenates, including phenolics, furans, esters; alkenes and alkanes, and nitrogenated compounds, which are decomposition products of lignin, cellulose, and proteins, respectively [15].

Previous studies on HTL of cattle manure showed that lignin and proteins in cattle manures lead to biocrudes with a more phenolic structure; these compounds may also contribute to char formation via 1,3-dipolar cycloaddition, Michael addition, amination, and oxidative polymerization [23,45], generating hydrochars with polyanilines, amines, and other nitrogenated and phenolic compounds. Similarly, Sudibyo et al. [37] reported that lignin decomposition under HTL conditions led to the formation of amides, phenoxyacids, quinones and azoles under alkaline conditions (pH 8), while acidic conditions (pH 3.5) promoted amination and hydroformylation of phenols. On the other hand, cellulose contributes to hydrochar formation mainly through furans, carboxylic acids and ketones. Sudibyo et al. [37] also noted that the ammonia released in the HTL AP contributed to forming pyrroles and other N-heterocycles in the hydrochar.

Regarding the effect of reaction temperature, He et al. [23] argue that increasing HTL temperatures would promote char and gas formation from biocrude's phenolic structures. From Fig. 8, it is observed that B300H contains a relatively higher content of nitrogenated compounds

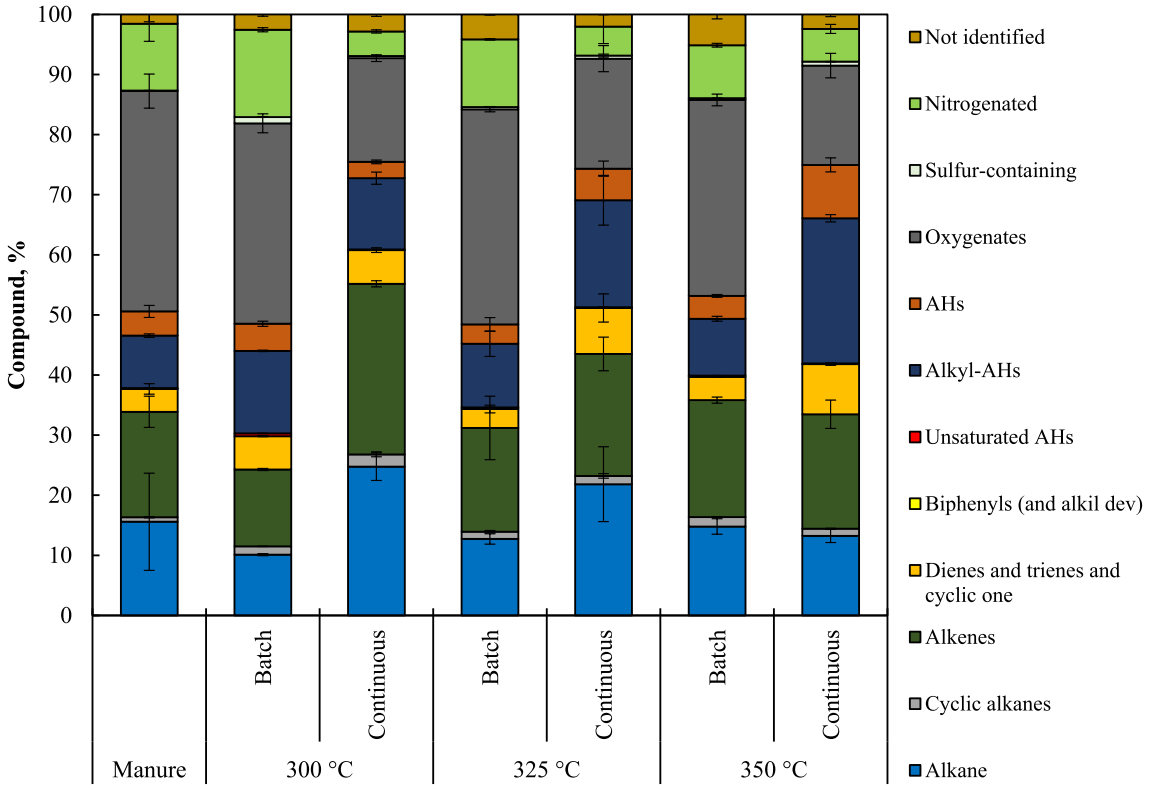

Fig. 8. Organic composition of pyrolysis products of cattle manure, continuous primary hydrochars and batch hydrochars from HTL at 300, 325 and 350 °C.

which are then reduced with increasing temperature. As regards the oxygenated compounds, the fraction remains stable at the three temperatures, although the phenolic content decreases with increasing reaction temperature, while more organic acids (acetic acid, hexadecanoic acid, octadecanoic acid) were detected with increasing temperature; in other words, there is a progressive shift in oxygenated compounds from phenolic to acidic with increasing HTL temperature.

On the other hand, continuous hydrochars had a lower amount of nitrogenated and oxygenated compounds throughout the three reaction temperatures. This is in alignment with the N and O content in Table 3. This suggests that a considerable fraction of nitrogenated and oxygenated compounds form after the primary char was collected, probably during the reaction cool down phase, thus they are detected in the batch but not in the continuous primary char. Further analysis of the continuous secondary char would shed light on this aspect. The largest contributors to the volatile organic fraction in continuous hydrochars are alkanes and alkenes which represent over 50% at 300 °C but show a steady decrease at 325 and 350 °C, being replaced by aromatic structures with alkyl substituents. The opposite trend was observed for batch hydrochars.

4. Conclusions

Understanding the differences between the hydrochar characteristics in batch and continuous HTL is key to determining suitable valorisation routes for this byproduct, which is highly important given its high nutrient load and for the implementation of industrial scale HTL solutions. In this study, the hydrochar produced from both batch and continuous HTL at 300, 325 and 350 °C was thoroughly characterised, elucidating their main differences and shedding light on the operational parameters that may cause them. For continuous reaction it was possible to separate primary and secondary char and infer their formation mechanisms.

In general, batch hydrochars yields were higher and temperature dependant, while continuous hydrochar yields (primary and secondary combined) were lower. The ash content of batch hydrochars was lower than for continuous primary chars demonstrating that the in-line char separator used in the continuous reactions effectively removed inorganic impurities at reaction conditions and producing a cleaner biocrude. Moreover, less C migrated to the solids from continuous HTL, indicating that removing inorganics reduces char formation during HTL.

The nutrients distribution in the HTL products did not reveal significant differences in the char composition but showed batch biocrudes contained more inorganic impurities such as Na, K and Fe, while on Fe was present in continuous biocrudes.

Organic-wise, the batch hydrochars showed a higher presence of oxygenated and nitrogenated compounds while the continuous primary chars had a higher share of alkanes and alkenes. Both chars showed contrasting trends with respect to the reaction temperature.

These differences may imply that batch reactions may not serve as indicators, in terms of hydrochar characteristics, for HTL upscaling to industrial plants.

Funding

This work was supported by the European Research Council (ERC) under the European Union's Horizon 2020 research and innovation programme [grant number 849841].

CRediT authorship contribution statement

María J. Rivas-Arrieta: Writing – original draft, Methodology, Investigation, Formal analysis, Data curation, Conceptualization. **Cristian Torri:** Writing – review & editing, Formal analysis. **Alessandro Girolamo Rombolà:** Writing – review & editing, Formal analysis. **Patrick Biller:** Writing – review & editing, Supervision, Funding acquisition, Conceptualization.

Data availability

Data will be made available on request.

References

[1] J. Lorimor, W. Powers, A. Sutton, Manure characteristics MWPS-18, Manure Manag. Syst. Ser. (2004) 1–24, https://doi.org/10.1201/9781420006537.ch3.
[2] J. Köninger, E. Lugato, P. Panagos, M. Kochupillai, A. Orgiazzi, M.J.I. Briones, Manure management and soil biodiversity: towards more sustainable food systems in the EU, Agric. Syst. 194 (2021), https://doi.org/10.1016/j.agsy.2021.103251.
[3] European Commission, Ensuring Availability and Affordability of Fertilisers, 2022. https://agriculture.ec.europa.eu/common-agricultural-policy/agri-food-supply-chain/ensuring-availability-and-affordability-fertilisers_en#fertiliser-trade. (Accessed 4 December 2023).
[4] D. Lachos-Perez, P. César Torres-Mayanga, E.R. Abaide, G.L. Zabot, F. De Castilhos, Hydrothermal carbonization and Liquefaction: differences, progress, challenges, and opportunities, Bioresour. Technol. 343 (2022), https://doi.org/10.1016/j.biortech.2021.126084.
[5] J. Lu, J. Zhang, Z. Zhu, Y. Zhang, Y. Zhao, R. Li, J. Watson, B. Li, Z. Liu, Simultaneous production of biocrude oil and recovery of nutrients and metals from human feces via hydrothermal liquefaction, Energy Convers. Manag. 134 (2017) 340–346, https://doi.org/10.1016/j.enconman.2016.12.052.
[6] M. El Bast, N. Allam, Y. Abou Msallem, S. Awad, K. Loubar, A review on continuous biomass hydrothermal liquefaction systems: process design and operating parameters effects on biocrude, J. Energy Inst. 108 (2023) 101260, https://doi.org/10.1016/j.joei.2023.101260.
[7] H. Shahbeik, H. Kazemi Shariat Panahi, M. Dehhaghi, G.J. Guillemin, A. Fallahi, H. Hosseinzadeh-Bandbafha, H. Amiri, M. Rehan, D. Raikwar, H. Latine, B. Pandalone, B. Khoshnevisan, C. Sonne, L. Vaccaro, A.S. Nizami, V.K. Gupta, S. S. Lam, J. Pan, R. Luque, B. Sels, W. Peng, M. Tabatabaei, M. Aghbashlo, Biomass to biofuels using hydrothermal liquefaction: a comprehensive review, Renew. Sustain. Energy Rev. 189 (2024) 113976, https://doi.org/10.1016/j.rser.2023.113976.
[8] J. Lu, J. Watson, Z. Liu, Y. Wu, Elemental migration and transformation during hydrothermal liquefaction of biomass, J. Hazard Mater. 423 (2022) 126961, https://doi.org/10.1016/j.jhazmat.2021.126961.
[9] A. Matayeva, S.R. Rasmussen, P. Biller, Distribution of nutrients and phosphorus recovery in hydrothermal liquefaction of waste streams, Biomass Bioenergy 156 (2022) 106323, https://doi.org/10.1016/j.biombioe.2021.106323.
[10] F. Conti, S.S. Toor, T.H. Pedersen, T.H. Seehar, A.H. Nielsen, L.A. Rosendahl, Valorization of animal and human wastes through hydrothermal liquefaction for biocrude production and simultaneous recovery of nutrients, Energy Convers. Manag. 216 (2020) 112925, https://doi.org/10.1016/j.enconman.2020.112925.
[11] F. Conti, S.S. Toor, T.H. Pedersen, A.H. Nielsen, L.A. Rosendahl, Biocrude production and nutrients recovery through hydrothermal liquefaction of wastewater irrigated willow, Biomass Bioenergy 118 (2018) 24–31, https://doi.org/10.1016/j.biombioe.2018.07.012.
[12] M. Karbakhshravari, I.S.A. Abeysiriwardana-Arachchige, S.M. Henkanatte-Gedera, F. Cheng, C. Papelis, C.E. Brewer, N. Nirmalakhandan, Recovery of struvite from hydrothermally processed algal biomass cultivated in urban wastewaters, Resour. Conserv. Recycl. 163 (2020) 105089, https://doi.org/10.1016/j.resconrec.2020.105089.
[13] G.C. Becker, D. Wüst, H. Köhler, A. Lautenbach, A. Kruse, Novel approach of phosphate-reclamation as struvite from sewage sludge by utilising hydrothermal carbonization, J. Environ. Manag. 238 (2019) 119–125, https://doi.org/10.1016/j.jenvman.2019.02.121.
[14] E. Ovsyannikova, A. Kruse, G.C. Becker, Feedstock-dependent phosphate recovery in a pilot-scale hydrothermal liquefaction bio-crude production, Energies 13 (2020) 1–3, https://doi.org/10.3390/en13020379.
[15] D.C. Elliott, T.R. Hart, G.G. Neuenschwander, L.J. Rotness, G. Roesijadi, A. H. Zacher, J.K. Magnuson, Hydrothermal processing of macroalgal feedstocks in continuous-flow reactors, ACS Sustain. Chem. Eng. 2 (2014) 207–215, https://doi.org/10.1021/sc400251p.
[16] D.C. Elliott, T.R. Hart, A.J. Schmidt, G.G. Neuenschwander, L.J. Rotness, M. V. Olarte, A.H. Zacher, K.O. Albrecht, R.T. Hallen, J.E. Holladay, Process development for hydrothermal liquefaction of algae feedstocks in a continuous-flow reactor, Algal Res. 2 (2013) 445–454, https://doi.org/10.1016/j.algal.2013.08.005.
[17] H. Wang, M. Zhang, X. Han, Y. Zeng, C.C. Xu, Production of biocrude oils from various bio-feedstocks through hydrothermal liquefaction: comparison of batch and continuous-flow operations, Biomass Bioenergy 173 (2023) 106810, https://doi.org/10.1016/j.biombioe.2023.106810.
[18] M.H. Marzbali, J. Paz-Ferreiro, S. Kundu, M. Ramezani, P. Halder, S. Patel, T. White, S. Madapusi, K. Shah, Investigations into distribution and characterisation of products formed during hydrothermal carbonisation of paunch waste, J. Environ. Chem. Eng. 9 (2021) 104672, https://doi.org/10.1016/j.jece.2020.104672.
[19] R. Aniza, W.H. Chen, F.C. Yang, A. Pugazhendh, Y. Singh, Integrating Taguchi method and artificial neural network for predicting and maximizing biofuel production via torrefaction and pyrolysis, Bioresour. Technol. 343 (2022) 126140, https://doi.org/10.1016/j.biortech.2021.126140.

[20] S.A. Channiwala, P.P. Parikh, A unified correlation for estimating HHV of solid, liquid and gaseous fuels, Fuel 81 (2002) 1051–1063, https://doi.org/10.1016/S0016-2361(01)00131-4.
[21] K. Wu, Y. Gao, G. Zhu, J. Zhu, Q. Yuan, Y. Chen, M. Cai, L. Feng, Characterization of dairy manure hydrochar and aqueous phase products generated by hydrothermal carbonization at different temperatures, J. Anal. Appl. Pyrolysis 127 (2017) 335–342, https://doi.org/10.1016/j.jaap.2017.07.017.
[22] J.S. Dos Passos, A. Matayeva, P. Biller, Synergies during hydrothermal liquefaction of cow manure and wheat straw, J. Environ. Chem. Eng. 10 (2022) 108181, https://doi.org/10.1016/j.jece.2022.108181.
[23] S. He, J. Wang, Z. Cheng, H. Dong, B. Yan, G. Chen, Synergetic effect and primary reaction network of corn cob and cattle manure in single and mixed hydrothermal liquefaction, J. Anal. Appl. Pyrolysis 155 (2021) 105076, https://doi.org/10.1016/j.jaap.2021.105076.
[24] Q. Liu, R. Xu, C. Yan, L. Han, H. Lei, R. Ruan, X. Zhang, Fast hydrothermal co-liquefaction of corn stover and cow manure for biocrude and hydrochar production, Bioresour. Technol. 340 (2021) 125630, https://doi.org/10.1016/j.biortech.2021.125630.
[25] Q. Liu, G. Kong, G. Zhang, T. Cao, K. Wang, X. Zhang, L. Han, Recent advances in hydrothermal liquefaction of manure wastes into value-added products, Energy Convers. Manag. 292 (2023) 117392, https://doi.org/10.1016/j.enconman.2023.117392.
[26] Q. Liu, G. Zhang, M. Liu, G. Kong, R. Xu, L. Han, X. Zhang, Fast hydrothermal liquefaction coupled with homogeneous catalysts to valorize livestock manure for enhanced biocrude oil and hydrochar production, Renew. Energy 198 (2022) 521–533, https://doi.org/10.1016/j.renene.2022.08.090.
[27] P. Biller, R.B. Madsen, M. Klemmer, J. Becker, B.B. Iversen, M. Glasius, Effect of hydrothermal liquefaction aqueous phase recycling on bio-crude yields and composition, Bioresour. Technol. 220 (2016) 190–199, https://doi.org/10.1016/j.biortech.2016.08.053.
[28] F. Marrakchi, S. Sohail Toor, A. Haaning Nielsen, T. Helmer Pedersen, L. Aistrup Rosendahl, Bio-crude oils production from wheat stem under subcritical water conditions and batch adsorption of post-hydrothermal liquefaction aqueous phase onto activated hydrochars, Chem. Eng. J. 452 (2023) 1–11, https://doi.org/10.1016/j.cej.2022.139293.
[29] E. Lappa, P.S. Christensen, M. Klemmer, J. Becker, B.B. Iversen, Hydrothermal liquefaction of Miscanthus × Giganteus: preparation of the ideal feedstock, Biomass Bioenergy 87 (2016) 17–25, https://doi.org/10.1016/j.biombioe.2016.02.008.
[30] K. Kapusta, Effect of ultrasound pretreatment of municipal sewage sludge on characteristics of bio-oil from hydrothermal liquefaction process, Waste Manag. 78 (2018) 183–190, https://doi.org/10.1016/j.wasman.2018.05.043.
[31] P.A. Marrone, D.C. Elliott, J.M. Billing, R.T. Hallen, T.R. Hart, P. Kadota, J. C. Moeller, M.A. Randel, A.J. Schmidt, Bench-scale evaluation of hydrothermal processing technology for conversion of wastewater solids to fuels, Water Environ. Res. 90 (2018) 329–342, https://doi.org/10.2175/106143017x15131012152861.
[32] U. Ekpo, A.B. Ross, M.A. Camargo-Valero, P.T. Williams, A comparison of product yields and inorganic content in process streams following thermal hydrolysis and hydrothermal processing of microalgae, manure and digestate, Bioresour. Technol. 200 (2016) 951–960, https://doi.org/10.1016/j.biortech.2015.11.018.
[33] C. Wang, W. Zhu, H. Zhang, C. Chen, X. Fan, Y. Su, Char and tar formation during hydrothermal gasification of dewatered sewage sludge in subcritical and supercritical water: influence of reaction parameters and lumped reaction kinetics, Waste Manag. 100 (2019) 57–65, https://doi.org/10.1016/j.wasman.2019.09.011.
[34] M. Pecchi, M. Baratieri, A.R. Maag, J.L. Goldfarb, Uncovering the transition between hydrothermal carbonization and liquefaction via secondary char extraction: a case study using food waste, Waste Manag. 168 (2023) 281–289, https://doi.org/10.1016/j.wasman.2023.06.009.
[35] M. Volpe, L. Fiori, From olive waste to solid biofuel through hydrothermal carbonisation: the role of temperature and solid load on secondary char formation and hydrochar energy properties, J. Anal. Appl. Pyrolysis 124 (2017) 63–72, https://doi.org/10.1016/j.jaap.2017.02.022.
[36] T. Voisin, A. Erriguible, D. Ballenghien, D. Mateos, A. Kunegel, F. Cansell, C. Aymonier, Solubility of inorganic salts in sub- and supercritical hydrothermal environment: application to SCWO processes, J. Supercrit. Fluids 120 (2017) 18–31, https://doi.org/10.1016/j.supflu.2016.09.020.
[37] H. Sudibyo, J.W. Tester, Probing elemental speciation in hydrochar produced from hydrothermal liquefaction of anaerobic digestates using quantitative X-ray diffraction, Sustain. Energy Fuels 6 (2022) 5474–5490, https://doi.org/10.1039/d2se01092e.
[38] R. Ghadge, N. Nagwani, N. Saxena, S. Dasgupta, A. Sapre, Design and scale-up challenges in hydrothermal liquefaction process for biocrude production and its upgradation, Energy Convers. Manag. X. 14 (2022) 100223, https://doi.org/10.1016/j.ecmx.2022.100223.
[39] Y. Deng, T. Zhang, J. Clark, T. Aminabhavi, A. Kruse, D.C.W. Tsang, B.K. Sharma, F. Zhang, H. Ren, Mechanisms and modelling of phosphorus solid-liquid transformation during the hydrothermal processing of swine manure, Green Chem. 22 (2020) 5628–5638, https://doi.org/10.1039/d0gc01281e.
[40] H. Wang, Z. Yang, X. Li, Y. Liu, Distribution and transformation behaviors of heavy metals and phosphorus during hydrothermal carbonization of sewage sludge, Environ. Sci. Pollut. Res. 27 (2020) 17109–17122, https://doi.org/10.1007/s11356-020-08098-4.
[41] F. He, X. Li, F. Behrendt, T. Schliermann, J. Shi, Y. Liu, Critical changes of inorganics during combustion of herbaceous biomass displayed in its water soluble fractions, Fuel Process, Technol. 198 (2020) 106231, https://doi.org/10.1016/j.fuproc.2019.106231.
[42] M. Schubert, J.W. Regler, F. Vogel, Continuous salt precipitation and separation from supercritical water. Part 2. Type 2 salts and mixtures of two salts, J. Supercrit. Fluids 52 (2010) 113–124, https://doi.org/10.1016/j.supflu.2009.10.003.
[43] J. Jiang, P.E. Savage, Using solvents to reduce the metal content in crude bio-oil from hydrothermal liquefaction of microalgae, Ind. Eng. Chem. Res. 58 (2019) 22488–22496, https://doi.org/10.1021/acs.iecr.9b03497.
[44] S.P.J. Higson, Analytical Chemistry, OUP, Oxford, 2003.
[45] H. Sudibyo, J.W. Tester, Sustainable resource recovery from dairy waste: a case study of hydrothermal Co-liquefaction of acid whey and anaerobic digestate mixture, Energy Fuel. 37 (2023) 2897–2911, https://doi.org/10.1021/acs.energyfuels.2c03860.